A COMPARISON OF LBW AND GTAW PROCESSES IN MINIATURE CLOSURE WELDS*

G. A. Knorovsky, P. W. Fuerschbach, S. E. Gianoulakis, S. N. Burchett,
Sandia National Laboratories
Albuquerque, NM 87185

Abstract

When small electronic components with glass-to-metal seals are closure welded, residual stresses developed in the glass are of concern. If these stresses exceed allowable tensile levels, the resulting weld-induced seal failure may cause the entire component to be scrapped or reworked at substantial cost. Conventional wisdom says the best welding process for these applications is that which provides the least heat input, and that Laser Beam Welding (LBW) provides less heat input than Gas Tungsten Arc Welding (GTAW); however, other concerns such as weld fit-up, part variability, and material weldability can modify the final choice of a welding process. In this paper we compare the characteristic levels of heat input and the residual stresses generated in the glass seals for the two processes (as calculated by 3D Finite Element Analysis) as a function of heat input and travel speed, and contrast some of the other manufacturing decisions that must be made to choose a production process. The geometry chosen is a standing edge corner weld in a cylindrical container about 20 mm diameter by 35 mm tall. Four metal pins are glassed into the part lid. The stresses calculated to result from continuous wave CO_2 LBW are compared with those that result from GTAW. The total energy required by the laser weld is significantly less (by 9 - 76%) than for the equivalent size GTA weld. The energy input required for a given size weld is inversely proportional to the travel speed, but approaches a saturation level as the travel speed increases. LBW travel speeds ranging from 10mm/sec to 50mm/sec were examined. The analysis of the laser welding process reveals nearly concentric isotherms advancing through the array of glass seals in the part lid. A similar analysis of the GTA process reveals more of a spiral arrangement of isotherms due to the much slower travel speed (5.8mm/sec). For the GTAW process, the effect of an Aluminum heat sink was also investigated. We will also include practical results obtained from actual components.

*This work performed at Sandia National Laboratories supported by the U.S. Dept. of Energy under contract number DE-AC04-94AL85000.

HERMETIC CONTAINERS PROVIDE an environmental barrier which ensures long life and reliability for many types of electronic devices used in modern technology. A closure weld on the package is normally one of the last manufacturing steps. When glass-to-metal seals are near the closure weld, the resulting thermal stresses developed in the glass are of concern. If these stresses exceed allowable tensile levels, the glass will crack, possibly resulting in loss of hermeticity. Failure of a seal typically dictates that the entire component be scrapped or reworked, often at substantial cost to the manufacturer. Hence, understanding how welding process parameters affect the stresses in the seals is desirable for development of an optimum weld schedule. Without this understanding, a qualification process with a statistically significant number of test specimens must be used to devise an acceptable weld. This trial and error process has been used successfully in the past; however, as electrical components being welded are becoming smaller and more complex, and testing more expensive, a more efficient means of optimizing the welding process is of increasing importance.

There are several approaches that can be taken to minimize the possibility of cracking the glass seals. These approaches include designing special weld joint geometries which act to minimize the required heat input, using high power density, low-total heat input welding processes such as laser and electron beam welding, keeping the seals as far as possible from the closure weld, using higher strength ceramic- or glass-ceramic-to-metal sealing procedures, and process optimization.

This paper examines in some detail the effects of heat input and travel speed, choosing values appropriate to continuous wave CO_2 Laser Beam Weld (LBW) and Gas Tungsten Arc Weld (GTAW) processes. The use of heat sinks with the slower travel speed GTAW process is also examined. A comprehensive three-dimensional numerical investigation was used to study the effect of heat source travel speed on temperatures and resulting thermal stresses in a small thermal battery during closure welding. This numerical simulation was guided by calorimetric-based experimentation we have conducted in our laboratory over the past several years on both GTAW and LBW processes [1] and which is referred to

elsewhere in this conference. Even though the LBW process may offer advantages with respect to heat input, it may still not be chosen given the complete set of constraints; we will discuss in some detail some of the manufacturing tradeoffs which govern the final process choice.

Computational Procedure

The geometry of the thermal battery lid and details of the glass-to-metal seals are shown in Figure 1. The materials used for the battery include: 304L stainless steel lid and casing, Corning 9010 glass insulators, and Alloy 52 (nominally Fe-52Ni) pins. The weld geometry simulated was a corner weld with a relief notch cut to provide a minimum ligament thickness equal to the casing thickness (0.40 mm). Experience has shown that this notch is beneficial in reducing the heat input necessary to produce a given size weld, as well as in balancing the melt between the lid and case. It also reduces the restraint of the weld, rendering it less susceptible to hot tearing. The weld begins adjacent to one of the seals and proceeds around the lid circumference, ending with 15 degrees of overlap.

To calculate the temperatures and stresses a one-way coupled thermal-mechanical analysis was performed in two steps. Step 1 performed a transient 3D thermal analysis of the welding process. In step 2 the temperatures from step 1 were mapped onto the structural nodes as source terms to compute the thermally-induced stresses. The finite element meshes used for the thermal calculations are shown in Figures 2 and 3.

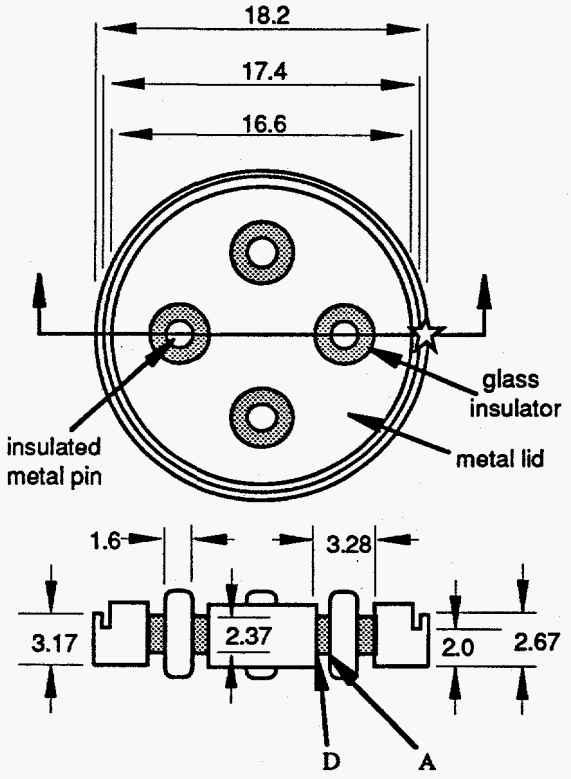

Figure 1 Schematic of thermal battery lid. All dimensions are in mm. Star indicates location of weld start. Letters indicate locations of maximum principal stresses plotted in subsequent figures.

The mesh for the LBW structural calculations was similar, but used increased mesh densities near the weld, in the lid near the seals, and within the seals. A total of 12376 8-node elements were in the thermal mesh and 34950 8-node elements were in the structural mesh. The LBW meshes were generated using P3/PATRAN and thermal calculations were performed using P/THERMAL [2] on a SUN SPARC10-51 workstation. Thermal calculations made for the GTAW process were done by JACQ and were meshed by GEN3D; they are reported in [3]. All structural analyses were performed using JAC3D [4] on a Cray Y-MP. JAC3D is a finite element code which calculates the non-linear quasi-static response of solids using the conjugate gradient method. JACQ [5] is a thermal code which also uses the conjugate gradient approach. The welding heat flux from the arc or laser was simulated by sequentially applying trapezoidal (vs time) surface or volume heat flux pulses, respectively, in 15 degree arcs along the path of the weld. Succeeding pulses overlapped at the temporal midpoint of the downslope/upslope ramps, which were of the same rate for a given weld. This provides continuity in the rate at which energy is provided to the part, closely representing the actual welding process. The time that the pulse was at full power was 80% for the laser and ~60% for GTAW. This scheme results in the proper amount of energy being deposited in each geometric arc. The total heat input to the material consisted of 25 equal magnitude pulses. This approach discretely models the continuous heat sources which travel around the lid. 15 degree arcs were shown by animation to adequately model the heat sources' continuous motion. The ramp time and duration of each pulse was determined based on the travel speed of the heat source. The magnitude of the pulses was based on the power input required by the part (see the next section).

Thermal conductivity values for the stainless steel header and casing were obtained from [6] and input as functions of temperature. Constant specific heat and density of 460 J/kgK and 7.817 x 10^{-6} kg/m^3 were used. The latent heat of fusion and vaporization were modeled by step changes in the specific heat over the transition regions between solid and liquid, and liquid and vapor respectively for the LBW case only. The material properties for the Alloy 52 pins and Corning 9010 glass insulators were obtained from vendor literature [7,8].

The boundary conditions in the LBW thermal model included natural convection and radiation to the surroundings. Since the purpose of this study was to examine the effect of travel speed on temperature and stresses, detailed convection and radiation models were not used. Rather, simple convection correlations for vertical surfaces [9] and gray body radiation relations [10] were used. The GTAW welds did not incorporate convective/radiative losses. For the no heat sink condition, insulated boundaries were used, while for the heat sink case, perfect coupling to the Al heat sinks was assumed at all part/heat sink interfaces.

Weld Schedules

Melting efficiency is a figure of merit for fusion welding which indicates how effectively the heat deposited into the workpiece is utilized. Melting efficiency is the ratio of the heat necessary to just melt the fusion zone to the heat absorbed by the workpiece. It is calculated by dividing the enthalpy of the weld volume ($\delta h \times V$ where V is the weld

volume and δh is the enthalpy required to raise a unit volume of material from ambient to the completely liquid state) by the net heat input. By this definition, superheating the fusion zone reduces the melting efficiency.

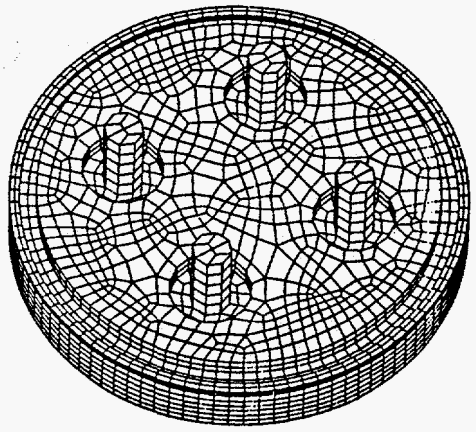

Figure 2a Lid Thermal mesh for LBW

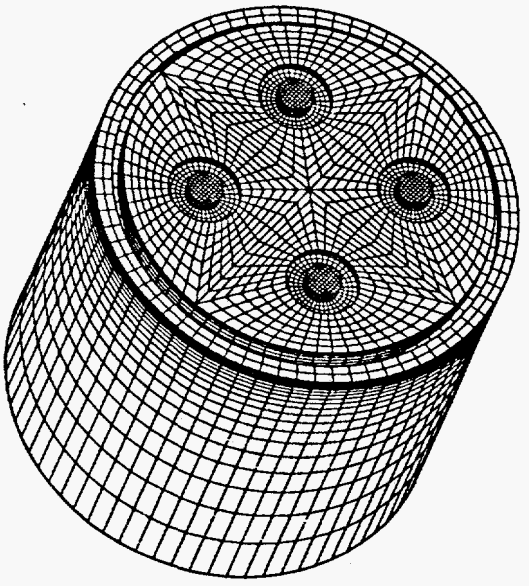

Figure 2b Lid and Casing Meshes for GTAW

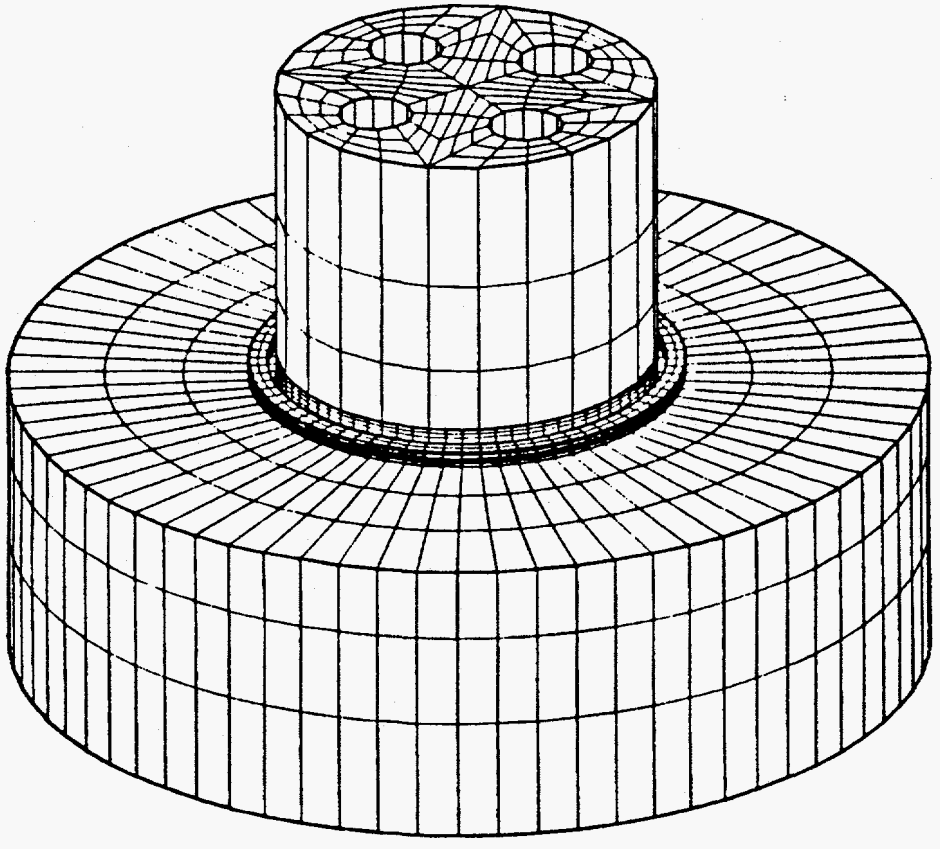

Figure 3 Heat sink meshes for GTAW

It is important to note that it is possible to produce welds that are equivalent in size and geometry but have unlike overall heat inputs and thermal histories because of variation in melting efficiency.

To simulate welds with varying melting efficiencies at equivalent penetration, a combination of empirical data relating penetration to irradiance and travel speed and a mathematical model for CO_2 laser welding [11] was employed to select input parameters. The desired weld penetration depth was determined using the empirical correlations for a suitable range of travel speeds. The model, which uses two dimensionless parameters that relate the cross sectional area of a laser weld to the travel speed and the net heat absorbed by the workpiece, was then used to select appropriate heat inputs and estimate the melting efficiency. The weld parameters selected are given in Table 1:

Table 1 - Weld parameters and efficiencies

Travel Speed (mm/sec) & Process	Laser Model-Estimated Absorbed Energy (J/rev)	Model - Estimated Melting Efficiency	FEM-Calculated Melting Efficiency
10 LBW	668	0.10-0.16	0.08
20 LBW	379	0.18-0.25	0.13
30 LBW	305	0.26-0.32	0.17
40 LBW	277	0.31-0.36	0.25
50 LBW	259	0.35-0.39	0.30
6 GTAW	1067	not applicable	0.04
6 GTAW (no H.S.)	737	0.06-0.08	0.08

The calculated cross sectional areas of the laser welds after about 180° of weld, were 0.12 (10-30 mm/s), 0.16 (40 mm/s) and 0.18 mm^2 (50 mm/s). The aim was 0.2 mm^2. The area increased with the faster welds, due to increased melting efficiency. The shape of the fusion zone was found to be nearly triangular. In contrast, the sizes and shapes of the GTAW welds were 0.16 and 0.21 mm^2, (with and without heatsink, respectively) and nearly rectangular. The fusion zone shape changess are caused by the differing methods of applying heat to the part. For the GTAW case a surface flux was applied across the entire width of the weld lip and casing while for LBW a volume flux was applied to the elements adjacent to the faying surface.

Thermal Analysis

The thermal battery, besides containing four glass-to-metal seals also contains a temperature sensitive igniter located under the lid at the center. Figure 4 shows the temperature histories of the center of the bottom side of the battery header during LBW and GTAW. Figure 5 shows the overall isotherms for the GTAW case after one complete revolution. The temperature histories at the top and bottom surface outermost nodes of the glass seals are shown in Figure 6, where it is seen that the pin next to the start/stop location (at 3 o'clock) reaches the highest temperature. Figure 7 shows the isotherms for 10mm/s, 30 mm/s and 50 mm/s laser welds after a complete revoltion.

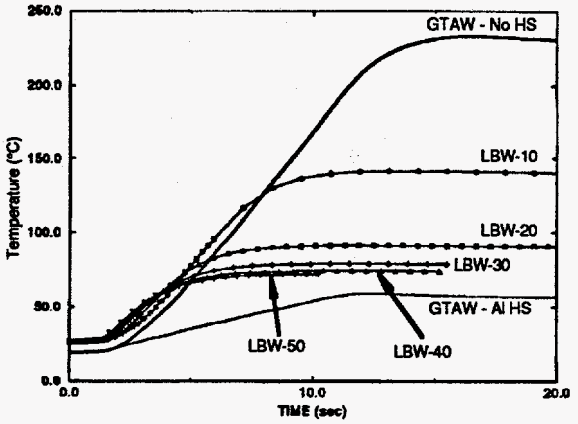

Figure 4 Temperatures at interior center of lid vs travel speed (in mm/s).

a)

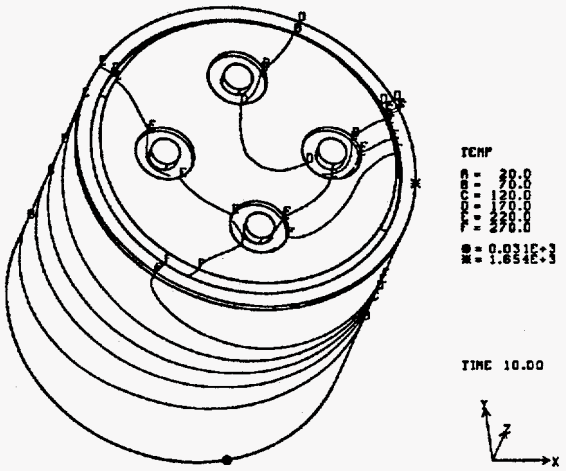

b)

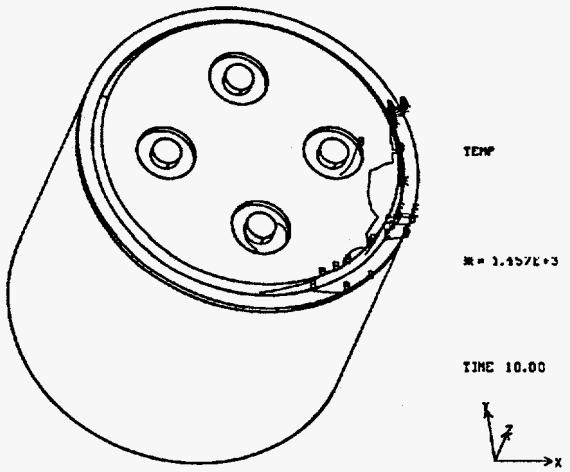

Figure 5 a) Temperature isotherms for GTAW at 1 full revolution (10 s), no heat sink. b) same but with Al heat sinks. * maximum temperature location, o minimum temperature location.

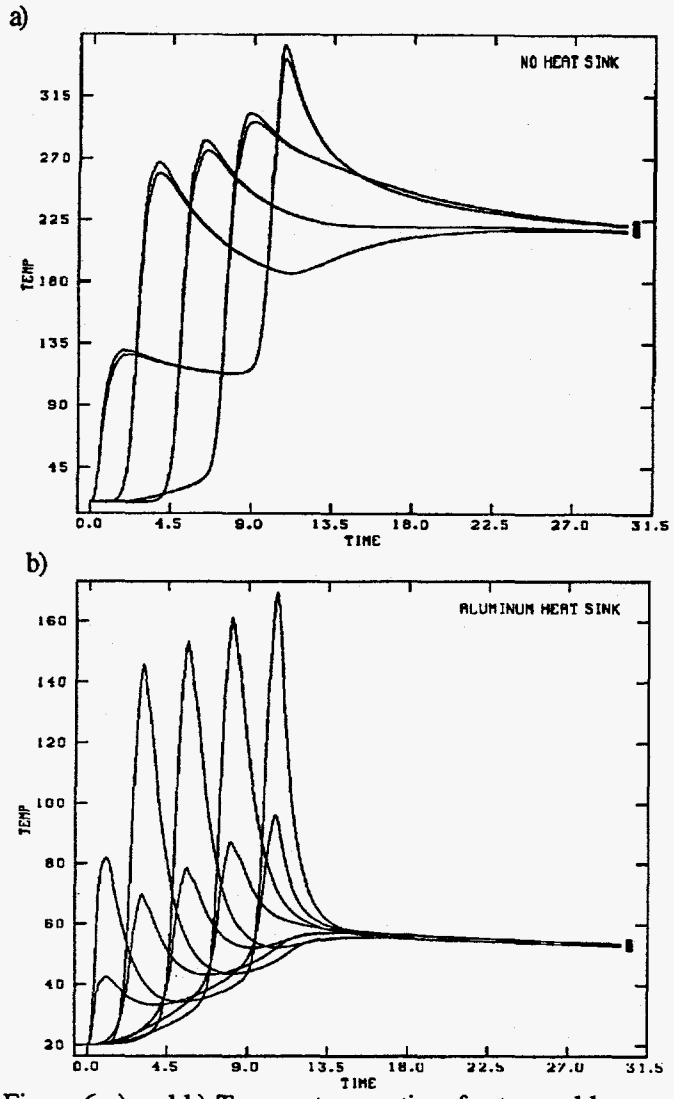

Figure 6 a) and b) Temperature vs time for top and bottom outermost glass nodes of each pin seen in Figures 5a & b.

The total energy input required for a given size weld was inversely related to the travel speed, but asymptotically approached a saturation level as the travel speed increased (see Table 1). As expected, the maximum temperatures reached at the center of the lid for the GTA welds were dramatically influenced by the heat sink, decreasing from a peak of 235°C to only 59°C even though the presence of the heat sink required a substantial increase in weld heat input. The heat sunk GTAW's maximum temperature is actually less than any of the non-heat sunk laser welds. The greatest qualitative difference noted in the isotherms as a function of travel speed is that they change from a broad to a narrow dispersion and become more concentric with the lid center. By the time the isotherms advance to the radial location of the pins, the higher travel speed welds have much flatter gradients, since much less heat was absorbed.

Stress Analysis

During the fabrication of lids containing glass-to-metal

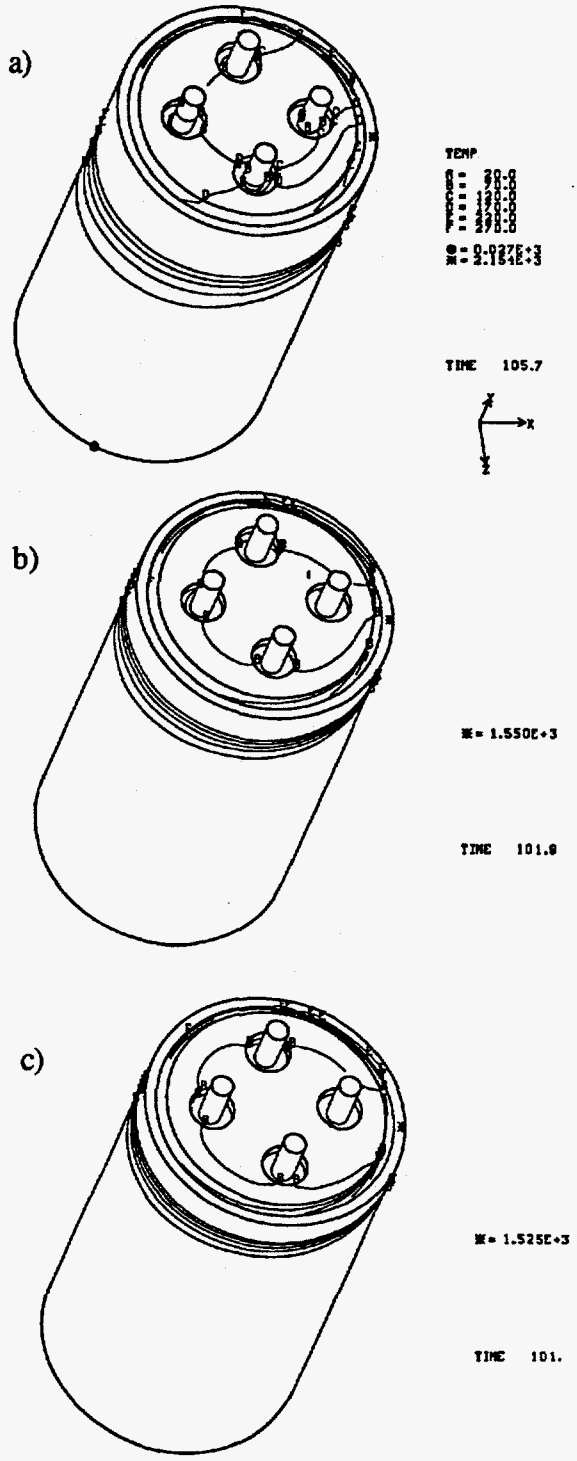

Figure 7 Temperature isotherms during laser welding after one full revolution a) 10 mm/s, b) 30 mm/s, c) 50 mm/s.

seals, stresses may be generated in the glass insulators, metal electrical connector pins, and the lid during the glassing operation due to differential thermal contraction of the glass and metal as the assembly cools to room temperature. Two design approaches are used to control the tensile stresses generated in the glass. One approach is to use glass and metal materials that have nearly the same thermal expansion

properties. This approach, referred to as a matched seal, produces a relatively stress-free state in the assembly after manufacture. The second approach

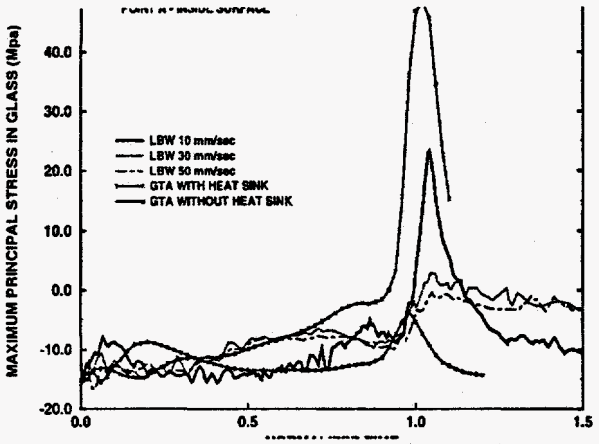

Figure 8 Maximum principal stress in glass @ location A for selected GTAW and LBW cases.

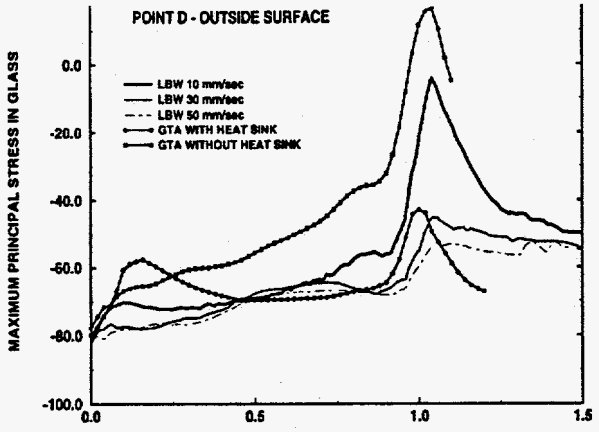

Figure 9 Maximum principal stress in glass @ location D for selected GTAW and LBW cases.

is to use a glass that has a thermal expansion coefficient that is less than that of the lid, but equal to that of the pins. This seal is called a compression seal because the glass near the housing is compressed during cooling. Design guidelines for coaxial compression pin seals have been developed [12] to minimize any tensile stress in the glass of a compression pin seal, thus enhancing the survivability of the glass in subsequent manufacturing or use environments. In this study, the material combination produces a compression pin seal. Therefore, the room temperature residual stress distribution must be determined prior to the weld simulation. This was accomplished by modifying the weld temperature history to include an initial stress-free temperature at the set-point temperature of the glass (445°C) and uniformly cooling to room temperature (27°C). The stresses in the assembly were then computed for both the manufacturing glassing operation and the subsequent weld operation. The glass was assumed to remain linear elastic below its set-point temperature. The metals were modeled as temperature dependent strain hardening elastic-plastic materials. At zones where the material exceeded the melt temperature, the deviatoric stresses were set to zero and the history state variables were reset to zero. As the temperatures in these elements cooled below the melting point, nonzero stresses were once again developed. Annealed values of the yield stress were used. Three of the LBW schedules were analyzed to examine stresses produced in the glass seals. Stress levels were found to decrease markedly between the 10 and 30 mm/sec travel speed cases. This is undoubtedly due to the halving of heat input. It is also clear that the overall residual compressive stresses introduced by the compression seals play a major role in keeping the peak tensile stresses below about 35MPa, a level generally associated with glass cracking. If the transient tensile stress peaks seen in Figures 8 & 9 had started from a stress free state, it is likely that cracked seals would result. Because of the lengthy computation time requirements for the stress model, the time of calculation was stopped at about 150% of the weld time. To see if this affected the final results, a subsequent uniform cool down to ambient was simulated for the 10 mm/sec weld (the highest heat input LBW). At the end of this cooldown, the residual stresses at the seals did not increase over levels seen either initially or during welding.

Manufacturability Issues

The thermal battery's internal construction presents a number of extenuating circumstances that affect the choice of welding process. As always, economic factors are extremely important, too.

First of all, the casing can be made either by deep drawing or by cutting from standard thin-wall tubing. In the former case, only one weld per assembly is necessary, whereas in the latter, two are required and a bottom lid is needed (without glass-to-metal seals). The decision here will generally be guided by the relative cost of piece part procurement vs welding. In general, if the production lot size is large enough, it will usually be less expensive to go with the two-piece design. Some tooling modifications or additions may need to be factored in, depending upon whether dedicated top & bottom weld stations are available or not. In both cases, the variability associated with forming will add to the tolerance on wall thickness and faying surface diameter to the detriment of consistent lid/casing radial fit-up.

Another important factor is that the contents of the battery are pressed together under a constant load in order to assure good electrical and thermal contact in operation. Since there are tolerance variations associated with each of the internal components, their total stack height varies appreciably, which in turn affects the axial positioning of the lid relative to the casing (a three-piece design allows the casing to be manually positioned to split this variability between the two welds, but poses manipulation challenges if the process is to be automated). The preload also facilitates the presence of a heat sink, since the pressure fixture can easily be designed to incorporate one. Actually, this requirement can cause some difficulty for the LBW process, as the load device may infringe upon the conical space requirements of the laser beam. This can be circumvented by a variety of measures, but

they do add slightly to the complexity of the tooling.

These factors aside, the increased productivity (high travel speed) and decreased stress generation (lower heat input) of the laser weld are offset by its smaller tolerance for poor fit-up (and more stringent piecepart tolerance requirements) and higher capital equipment, training and maintenance costs. If the gap between the lid and casing approaches the focussed beam diameter, a signficant reduction of energy transfer may happen, and actual damage to the internals of the part can occur because of the misplaced laser irradiance. Another difficulty is an inability to bridge the gap by the generally smaller LBW molten pool and failure to form a single weld bead. Yet another problem that may be encountered with LBW is that, being a high energy density process, it tends to produce more spatter balls than GTAW, and in some components, particularly those which have small and closely spaced electrical traces or close tolerance sliding mechanisms, spatter can cause functional failures. A final complication lies in the possibility of encountering hot cracking with some heats of 304L stainless steel which may solidify in a fully austenitic mode at high travel speeds. This would cause restrictions to be placed on the allowable chemistry of the piecepart materials (restricted ferrite number) and hence, added cost.

In general, for the relatively small production runs required by our customers, the vendors have chosen GTAW. With adequate process development and suitable heat sinks, cracking of the glass-to-metal seals has not been a significant limitation, which is in line with the stress calculation seen in an earlier section.

Discussion

As would be expected from physical intuition, the high power density LBW process requires substantially less heat input, particularly at fast travel speeds, and produces correspondingly lower residual stresses than the GTA weld. At a travel speed of 10 mm/s the stresses generated in the glass are at about the limit where glass cracking occurs, suggesting that higher travel speeds would be prudent for this application. However, the use of heat sinks is of great benefit. It must also be noted that the GTA weld simulated (though representative of an actual weld schedule) was not particularly efficient, and the process is capable of much higher melting efficiencies rivalling the LBW process. It is not at all unusual to see small autogenous GTA welds made at travel speeds of 12 mm/sec or greater.

The melting efficiencies predicted by the model and those calculated by FEM are in good if not great agreement. The model uses values of δh and thermal diffusivity which were determined from the literature, and which take into account the temperature dependence of density and the specific heat. The FEM material properties did not fully account for these factors, hence the range of model-estimated melting efficiencies in Table 1. The low value corresponds to the values used by the FEM material input, whereas the larger value corresponds to actual values. Though not tabulated, the empirically-based model-predicted weld cross-sectional areas and the FEM-calculated ones were also in similarly good agreement. Finally, actual LBW welds made in this geometry without heat sinks, at a travel speed of 32 mm/s (with 60% increased heat input over the 30 mm/s entry in Table 1) do not exhibit glass cracking.

Conclusions

1. Higher weld travel speeds clearly result in more efficient heat utilization, and require less overall heat input for a given size weld.
2. Lower heat inputs result in lower tensile stresses in the glass-to-metal seals in this model. A particularly dramatic reduction took place over the range of 10 to 20 mm/s travel speed.
3. Heat sinks can also act to reduce the tensile stresses, even though they may reduce the melting efficiency and increase the required heat input.
4. An empirically-based dimensionless parameter model gave good agreement with the FEM calculation of melting efficiency and weld size.
5. Practical considerations make the GTAW process competitive with LBW in circumstances where physical intuition would suggest otherwise.

References

1. Fuerschbach, P.W. and Knorovsky, G.A., "A Study of Melting Efficiency in Plasma Arc and Gas Tungsten Arc Welding," Welding Journal Research Supplement, 70, p287-s, (1991)
2. PDA Engineering, P3/PATRAN & P/THERMAL User's Manuals, Costa Mesa, CA, (1993)
3. Knorovsky, G.A. and Burchett, S.N., "The Effect of Heat Sinks in GTA Microwelding, *Proceedings of the 2nd International Conference on Trends in Welding Research*, ASM, pp 469-474,(1989)
4. Biffle, J.H., "JAC3D - A Three Dimensional Finite Element Computer Code for the Non-Linear Quasi-Static Response of Solids with the Conjugate Gradient Method," SAND87-1305, Sandia National Labs, (1993)
5. Personal communication with Biffle, J.H. Sandia National Laboratories, (1988)
6. Touloukian, Y.S., and Ho, C.Y., "Thermophysical Properties of Matter," Plenum Press, (1972)
7. Kohl, W.H. "Handbook of Materials and Techniques for Vaccuum Devices", Reinhold, 1967
8 Controlled Expansion Alloys Product Bulletin, Carpenter Technology Corp.
9. Incopera, F.P. and Dewitt, D.P., "Fundamentals of Heat and Mass Transfer, 3rd Ed., John Wiley & Sons, pp 541-554, (1990)
10. Siegel , R. and Howell , J.R., "Thermal Radiation Heat Transfer, 2nd Ed.", Hemisphere, pp. 236-246, (1981)
11. Fuerschbach , P.W., "Measurement and Prediction of Energy Transfer Efficiency in Laser Beam Welding," submitted for publication in Welding Journal,
12. Miller, J.D and Burchett, S.N. "Some Guidelines for the Mechanical Design of Coaxial Compression Seals," SAND82-0057, Sandia National Laboratories, (1982)